FORCE-INDENTATION CURVES OF SPHEROIDAL OBJECTS

Thesis Submitted in Partial Fulfillment of the Jay and Jeanie Schottenstein Honors Program

Benjamin Meir Goykadosh

Yeshiva College, Department of Physics

Under the supervision of Dr. Fredy Zypman, Physics

Yeshiva University

May 2021

Table of Contents

Abstract

Currently, there are many methods to determine the forces and energy necessary to deform cells. These methods, however, are slow and require testing outside of the body. In this paper, we propose a theoretical method to recover the energy and force vs. indentation curves produced by the deformation using an Atomic Force Microscope. The theory depends on parameters such as Young's modulus, object length, and Poisson's ratio, which are obtained by fitting our mathematical expressions to experimental force vs. indentation curves. Thus, our results provide a systematic way to measure those material parameters in general, but in particular in soft matter where the materials are highly heterogeneous and their properties are often dependent on external stresses.

Introduction

The Atomic Force Microscope (AFM) is one of the favored tools scientists use for micro and nano scale imaging and, of particular interest to the work presented here, soft biological nanoparticles, which include blood plasma, red blood cells, and white blood cells [1]. The AFM is able to achieve accuracies that standard microscopes cannot because of its capabilities of nano-meter spatial resolution and piconewton force sensitivity. In its most common version, the AFM utilizes a sensor made up of a cantilever rod with a tip at its hanging end. When the tip touches or interacts in non-contact with the surface of the particle under observation, the AFM records the tip height and the cantilever's angular deflection; these measurements then enable various quantities to be extracted via mathematical, computational postprocessing. Our main goal in this thesis is to develop a theoretical model of the sample under study which in turn allows us to compute the energy and force versus separation curves produced by the indentation of the sample by the AFM tip. This analysis will help us understand how external forces affect cell deformation. In the end, we hope that this knowledge will elucidate how certain physical parameters such as Young's Modulus and Poisson's Ratio affect the force/deformation connection.

The type of indentation just described and the corresponding force-distance measurement is uniquely suited for study via AFM. Due to its direct contact with the specimen, the AFM provides mechanical information about the cell that otherwise would not be accessible. We first

will provide a general equation that connects the energy and force with the indentation distance and the corresponding cell deformation.

Our proposed method would also be useful in determining cell contraction and overall shape. Cellular contraction, an ongoing research subject, is a phenomenon that drives various processes in the body. However, contracting cells only provide a small amount of force and stress, which are difficult to monitor inside the body [2]. Regardless of the progress made in recent years, there are still many limitations that prevent the determination of these forces. To solve these issues, study is often done in vitro, outside the body, which is incredibly difficult, cost prohibitive, and slow. Our proposed theoretical method would guide the experiments and thus provide a justification for the deployment of these scarce resources.

In this paper, I will first explain the theory and background to our work. I will explain the method in which we solved the general equations for computing the energy and the force on an object. Then I will share the results of our computations regarding specific examples. Finally, I will compare our theoretical model to actual experiments conducted in other universities to determine the accuracy of our theory.

Theory

The starting point for any theory of elasticity is Hooke's law, a foundational concept used in introductory physics courses as well as in advanced research. Developed by British physicist Robert Hooke [3] in 1678, he described it as "*ut tensio, sic vis"* or "the extension is proportional to the force." In its simplest form, Hooke's law is known as:

$$\vec{F} = -k\,\vec{x} \qquad (1)$$

where $\vec{F}$ is the force acting on the system, k is a proportionality constant dependent on the spring, and $\vec{x}$ is the displacement from equilibrium. Today's modern theory of elasticity generalizes Hooke's law to three dimensions such that the strain of an object is proportional to the stresses applied to it. These stresses and strains often are non-uniform fields within the body, and the proportionality factor is no longer a constant; instead, it is a tensor represented by the *elasticity matrix* [4]. For a three-dimensional system with non-uniform stresses and corresponding strains, Hooke's law is generalized as:

$$\vec{\sigma} = D\,\vec{\varepsilon} \qquad (2)$$

where $\vec{\sigma}$ is the stress vector field, D is the elasticity matrix, and $\vec{\varepsilon}$ is the local strain vector. These quantities are given explicitly by:

$$D = \begin{pmatrix} \lambda+2\mu & \lambda & \lambda & 0 & 0 & 0 \\ \lambda & \lambda+2\mu & \lambda & 0 & 0 & 0 \\ \lambda & \lambda & \lambda+2\mu & 0 & 0 & 0 \\ 0 & 0 & 0 & \mu & 0 & 0 \\ 0 & 0 & 0 & 0 & \mu & 0 \\ 0 & 0 & 0 & 0 & 0 & \mu \end{pmatrix} \qquad (3)$$

$$\vec{\sigma} = \begin{pmatrix} \sigma_x \\ \sigma_y \\ \sigma_z \\ \tau_{yz} \\ \tau_{xz} \\ \tau_{xy} \end{pmatrix} \qquad (4)$$

$$\vec{\varepsilon} = \begin{pmatrix} \varepsilon_x \\ \varepsilon_y \\ \varepsilon_z \\ \gamma_{yz} \\ \gamma_{xz} \\ \gamma_{xy} \end{pmatrix} \qquad (5)$$

In equation 3, λ and μ are the Lamè constants given in terms of the physically measurable quantities Young's Modulus Y and Poisson's ratio ν such that

$$\mu = \frac{Y}{2(1+\nu)} \qquad (6)$$

and

$$\lambda = \frac{Y\,\nu}{(1+\nu)(1-2\nu)} \qquad (7)$$

The scalar quantities σ_i, τ_{ij}, ε_i, and γ_{ij} are the normal stresses, the shear stresses, the normal strains, and the shear strains respectively. The stresses and strains can be calculated explicitly from local deformations in the system. Let $\vec{R}(\vec{x},\vec{y},\vec{z})$ be the deformation field of the cell in its equilibrium position produced by external forces. Then

$$\varepsilon_i = \frac{\partial R_i}{\partial x_i} \quad (8)$$

$$\gamma_{ij} = \frac{\partial R_i}{\partial x_j} + \frac{\partial R_j}{\partial x_i} \quad (9)$$

The strain, colloquially defined as the measure of the deformation in the material, is the dimensionless vector displacement component of a localized point relative to the same physical point of the body in unstressed equilibrium in units of the mesh side length. We will characterize the equilibrium, the unstrained starting shape of the body, by a parameter b_0, and its final, strained, position by *b*. The precise form of this characterization will be explained later, but we advance here that it will serve to model the indentation of a spheroid by a sharp pin. Therefore, the transformation $b_0 \rightarrow b$ induces the vector displacement for the strain at all points within the body. We propose in this thesis to build the strains $\vec{\varepsilon}$ from the transformation $b_0 \rightarrow b$ to model how the system deforms and its deformation field, which would then determine the energy and the concomitant force of that deformation. We will present a system of equations that determines the shape of the object before and after this indentation. Utilizing these equations, we can then use equations (8) and (9) to build the strain vector ($\vec{\varepsilon}$). This strain vector multiplied by the matrix D (Equation 3) returns the stress on the object, which expresses the internal forces that particles in a material exert on their neighboring particles.

In order to define $\vec{\sigma}$ and $\vec{\varepsilon}$, we first need to construct the system of equations to define the shape of the body. To model the system, by adding a *depth-parameter* b we modified a cardioid [5] such that the individual components of $\vec{R}(x, y, z)$ can be modeled as:

$$\vec{x} = L\ (2\ a\ Sin[\theta]\{1 + b\ a\ Cos[\theta]\})\ Cos[\phi] \quad (10)$$

$$\vec{y} = L\ (2\ a\ Sin[\theta]\{1 + b\ a\ Cos[\theta]\})\ Sin[\phi] \quad (11)$$

$$\vec{z} = L\ (2\ \{1 + b\ a\} - 2\ a\ Cos[\theta]\{1 + b\ a\ Cos[\theta]\} + 2\ b\ a\ (a - 1)) \quad (12)$$

The cardioid corresponds to setting b to zero in equations (10) through (12). By introducing the parameter *b*, we achieve the following properties for the object's shape. First, the deformation is larger at the object's surface (a =1). As a is reduced from one toward zero, the strain diminishes. That is, bulk points sense the indentation to a lesser extent than surface points do. Second, towards the surface, points close to the indenter ($\theta = \pi$) deform more than those close to the

substrate. Third, the sharp indenter produces a cusp at the contact point. As complete as this description is, and as rich in physical content, we appreciate the possibility of pushing the model further toward physical agreement. For example, when dealing with discrepancies between theory and reality, one consideration is the reality that at some small scale, tips can no longer be infinitely acute and form a finite, blunt surface. This idea, however, will not be pursued any further in this study. We leave it as an open problem.

In this model, L is a constant dependent on the linear dimensions of the object, a is a deformed variable radial coordinate between 0 and 1, and θ and ϕ are variable coordinates in the polar plane with θ having a range between 0 and π and ϕ having a range of 0 and 2π. Most importantly, b is the shape parameter and is related to the indentation deformation (Figure 1, 2). The parameter b is introduced, as explained, in such a way that the deformation of the object will be enhanced at its boundary while not affecting substantially the center of the body (see Figures 1 and 2). Taking the Jacobian of the system for the variables a, θ,and ϕ and integrating it in a, θ, and ϕ returns a volume of:

$$Volume = \int_0^1 \int_0^\pi \int_0^{2\pi} J \; d\phi \; d\theta \; da \rightarrow Volume = \frac{32}{3}(1 + b^2)L^3\pi \quad (13)$$

Taking the cube root of the result from equation (13) and dividing equations 10, 11, and 12 by the cube root of this result normalizes the volume of the system. This gives us:

$$\vec{x} = L\,(2\,a\,Sin[\theta]\{1 + b\,a\,Cos[\theta]\})\,Cos[\phi] \quad (14)$$

$$\vec{y} = L\,(2\,a\,Sin[\theta]\{1 + b\,a\,Cos[\theta]\})\,Sin[\phi] \quad (15)$$

$$\vec{z} = L\,(2\,\{1 + b\,a\} - 2\,a\,Cos[\theta]\{1 + b\,a\,Cos[\theta]\} + 2\,b\,a\,(a - 1)) \quad (16)$$

Using these new equations, we take the new Jacobian of this system and integrate again in a, θ, and ϕ. This returns a volume of L^3 which represents a successful calibration for the volume.

Using this calibration, we can now solve for the various values of R_i for equations (8) and (9). R_i is given by

$$R_i = R_i(b = b) - R_i(b = b_0) \quad (17)$$

where b is the variable deformation parameter and b_0 is the starting value of the deformation parameter as discussed above. We will take in this work that 0 < b0 < b < 1 (values of b > 1 give double valued shape boundaries which are not physical).

One issue with the framework described above is that it defines R as a function of $\vec{R}(x, y, z)$ when it is more naturally given in deformed spherical coordinates a, θ, and ϕ. To bridge this difference, we solved for $\vec{\varepsilon}$ using Cramer's rule for linear equations such that:

$$\begin{matrix} W_1 & X_1 & Y_1 & Z_1 \\ W_2 = & X_2 & Y_2 & Z_2 \\ W_3 & X_3 & Y_3 & Z_3 \end{matrix} \qquad (18)$$

where W_1 is $\frac{\partial R_i}{\partial a}$, W_2 is $\frac{\partial R_i}{\partial \theta}$, and W_3 is $\frac{\partial R_i}{\partial \phi}$. X_i is the derivative of equation (10) with regards to a, θ, and ϕ respectively, with similar calculations for Y_i and Z_i. $\overrightarrow{\varepsilon_i}$ is calculated as:

$$\overrightarrow{\varepsilon_i} = \frac{\det [A_i]}{\det [A]} \qquad (19)$$

where A_i is the matrix formed by replacing the i-th column of A by the column vector W. We also utilize this method to solve for the various γ_{ij}. Instead of using equation (9), we reinterpret it using Cramer's method from equation (16) such that:

$$\gamma_{ij} = \frac{\det [A_{ij}]}{\det [A]} + \frac{\det [A_{ji}]}{\det [A]} \qquad (20)$$

with similar calculations done for γ_{ik} and γ_{jk}.

Now that we can construct $\vec{\varepsilon}$, and by extension $\vec{\sigma}$, we can evaluate the energy of the system. The system of equations modeled by $\vec{R}(\vec{x}, \vec{y}, \vec{z})$ are used to solve for $\vec{\sigma}, D,$ and $\vec{\varepsilon}$ as discussed before. The energy (E_s) relates to these parameters such that:

$$E_s = \frac{1}{2} \iiint_{Volume} (\vec{\sigma} \cdot \vec{\varepsilon})\, dV \qquad (21)$$

Therefore, for a given initial condition b_0 and a deformation b, we can build the equations necessary to compute E_s.

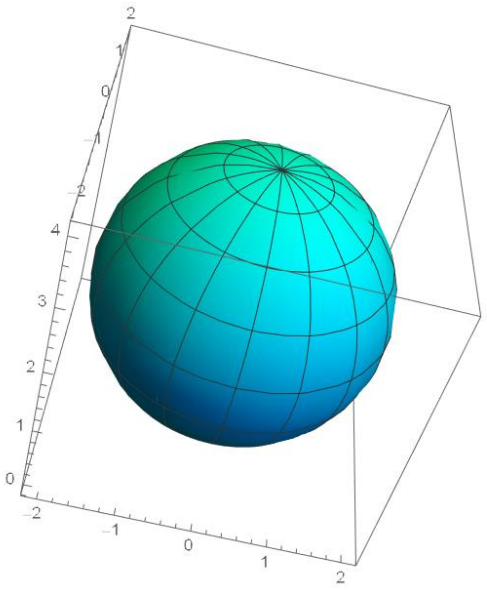

Figure 1: When $\vec{R}(\vec{x},\vec{y},\vec{z})$ is plotted over the ranges of $\theta = [-\pi,\pi]$ and $\phi = [0,2\pi]$ and a = 1, b = 0, we recover a cardioid deformed such that it is a sphere. This sphere can be an accurate model for pre-stressed white blood cells.

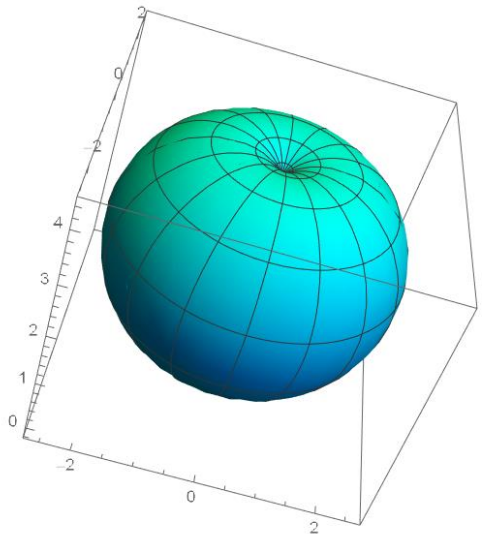

Figure 2: $\vec{R}(\vec{x},\vec{y},\vec{z})$ is plotted over the ranges of $\theta = [-\pi,\pi]$ and $\phi = [0,2\pi]$ and a = 1, b = .9, we recover a standard three-dimensional cardioid. This deformation accurately models a sphere under the influence of a cantilever point stress.

As briefly discussed above, the parameter b models an indentation by a sharp pin where transformation $b \to b_0$ induces the vector displacement for the strain at all points within the body. The equilibrium will be characterized as the unstrained starting shape of the body defined by parameter b_0 and its final, strained position by b. Both b_0 and b can take values between 0 and 1, provided that $b_0 < b$.[1] The parameter b is important based on how it relates to the indentation parameter *S*. *S* is obtained by determining the deformation the cell underwent from the point force. *S* is the change in position in the cell as the shape undergoes its deformation from the point force. The shape of the object is determined by utilizing equations 14, 15, and 16 and setting the parameter a to 1 and θ to π.[2] These values determine the overall shape of the object.

[1] Should b_0 be greater than b, this would indicate the object was actually becoming unstressed as the pin is being removed.

[2] ϕ can be set to zero since $\theta = \pi$ regardless of ϕ.

Under this determination, the X and Y dimensions (Equations 14 and 15) will be zero. However, the Z dimension (equation 16) returns the following value:

$$\frac{L\left(\frac{6}{\pi}\right)^{\frac{1}{3}}}{(1+b^2)^{\frac{1}{3}}} \quad (22)$$

This equation shows us where the point of the Z dimension is at any deformation b. Since *S* is defined by the change in the deformation, we take equation (22) at the initial position b_0 and subtract it by the final position *b*. This leads to *S* being defined as:

$$S = \frac{L(\frac{6}{\pi})^{\frac{1}{3}}}{(1+{b_0}^2)^{\frac{1}{3}}} - \frac{L\left(\frac{6}{\pi}\right)^{\frac{1}{3}}}{(1+b^2)^{\frac{1}{3}}} \quad (23)$$

Using this definition of *S*, we can now determine the force of the indentation. Classically, the force is defined as:

$$F(x) = -\frac{dU}{dx} \quad (24)$$

Where F(x) is the force on the object and $\frac{dU}{dx}$ is the change in energy, usually over time or a distance. In our experiment, this would mean that the force is determined by the change in E_s over the distance indented, *S*. Therefore, F would be defined as:

$$F(S) = -\frac{dE_s}{dS} \quad (25)$$

However, our original conditions (equations 14, 15, 16) are in terms of ***b*****,** not *S*. Therefore, we calculate the force required to indent the sphere by:

$$F(S) = -\frac{dE_s}{db}\frac{db}{dS} \quad (26)$$

where $\frac{db}{dS}$ is solved by solving Equation 23 for b and taking the derivative of the result with respect to S.[3]

Comparison with Experiments

Using the methods described above and using Mathematica in algebra mode, we were able to find a general method for the energy of the system.[4]

$$
\begin{aligned}
E_S = & \\
& -\Big(\big(L^3 Y \\
& \Big(8\,b\,\big(6\,b\,\left(1+b^2\right)^{2/3} b0\,(679-121\,\nu)+768\,b^5\,\left(1+b^2\right)^{1/3} b0\,\left(\left(1+b^2\right)^{1/3}-2\,\left(1+b0^2\right)^{1/3}\right)\,(1+\nu)+384\,b^6\,\left(1+b0^2\right)^{1/3}\left(-2\,\left(1+b^2\right)^{1/3}+3\,\left(1+b0^2\right)^{1/3}\right)\,(1+\nu)+ \\
& \quad 16\,b^3\,\left(1+b^2\right)^{2/3} b0\,(59+112\,\nu)+3\,\left(1+b^2\right)^{2/3} b0^2\,(-679+121\,\nu)-b^2\,\left(1+b^2\right)^{2/3}\left(2037-363\,\nu+8\,b0^2\,(59+112\,\nu)\right)+ \\
& \quad 8\,b^4\,\left(85\,\left(1+b^2\right)^{2/3}+16\,\left(-18\,\left(1+b^2\right)^{1/3}\left(1+b0^2\right)^{1/3}+9\,\left(1+b0^2\right)^{2/3}+2\,\left(1+b^2\right)^{2/3}\nu-18\,\left(1+b^2\right)^{1/3}\left(1+b0^2\right)^{1/3}\nu+9\,\left(1+b0^2\right)^{2/3}\nu+ \right.\right. \\
& \quad \left.\left. 3\,\left(1+b^2\right)^{2/3} b0^2\,(1+\nu)\right)\right)-6\,\left(1+b^2\right)^{2/3}\,(b-b0)^2\,\left(281+768\,b^2\,\left(-2+b^2\right)\,(-1+\nu)+889\,\nu\right)\,\text{ArcTanh}[b]- \\
& \quad 3\,\left(1+b^2\right)^{2/3}\,(b-b0)^2\left(96\,b^4\,(-1+\nu)+9\,\sqrt{9+16\,b^2}\,(37+5\,\nu)-8\,b^2\left(135-14\,\sqrt{9+16\,b^2}+5\,\sqrt{9+16\,b^2}\,\nu\right)\right)\text{Log}\left[-1-4\,b+\sqrt{9+16\,b^2}\right]+ \\
& \quad 3\,\left(1+b^2\right)^{2/3}\,(b-b0)^2\left(\left(96\,b^4\,(-1+\nu)-9\,\sqrt{9+16\,b^2}\,(37+5\,\nu)+8\,b^2\left(-135-14\,\sqrt{9+16\,b^2}+5\,\sqrt{9+16\,b^2}\,\nu\right)\right)\text{Log}\left[1-4\,b+\sqrt{9+16\,b^2}\right]+ \right. \\
& \quad \left.\left(96\,b^4\,(-1+\nu)+9\,\sqrt{9+16\,b^2}\,(37+5\,\nu)-8\,b^2\left(135-14\,\sqrt{9+16\,b^2}+5\,\sqrt{9+16\,b^2}\,\nu\right)\right)\text{Log}\left[-1+4\,b+\sqrt{9+16\,b^2}\right]+ \right. \\
& \quad \left.\left.\left(-96\,b^4\,(-1+\nu)+9\,\sqrt{9+16\,b^2}\,(37+5\,\nu)+8\,b^2\left(135+14\,\sqrt{9+16\,b^2}-5\,\sqrt{9+16\,b^2}\,\nu\right)\right)\text{Log}\left[1+4\,b+\sqrt{9+16\,b^2}\right]\right)\right)\Big/ \\
& \left(6144\,b^5\,\left(1+b^2\right)\,\left(1+b0^2\right)^{2/3}\,(1+\nu)\,(-1+2\,\nu)\right)\Big);
\end{aligned}
$$

While the equation is cumbersome, it can simply be cut and pasted for future use. It saves the user the need to do numerical integrations. This equation allows us to calculate the energy stored in the body, and by extension the force, as a function of the indentation s (connected to the shape parameter b, see equation 23). Y, L, υ, and b_0 are all constants that are material dependent. As an example, we calculated the force on an object with parameters $b_0 = 0, \upsilon = 0.25$ and arbitrary values of L and Y (Figure 3). We see that for small indentations the force-indentation curve quickly grows, then becomes linear for some distance. This matches our original expectations. The physical indentation of a cell can be modeled using this equation. The initial rapid polynomial growth represents the surface tensions opposing the effect of the indenter. The trend linearizes once the surface tension ruptures. The final rapid growth is where the cell approaches maximum compression. For example, imagine pushing with your thumb against a ball. At first it may be difficult to push down, perhaps because of some microscopic architecture that makes the

[3] One issue that arose with this method is that it used a lot of computing power and time to solve these equations directly. Therefore, we utilized a numeric approach for certain values. The code for this method can be found in Appendix 1.

[4] The equation for force is incredibly long and unable to be simplified. Hence, the code is reproduced in Appendix 1 for convenience. It runs very quickly in Mathematica and allows us to compute the force from the energy of indentation incredibly well.

equilibrium position a strong energy minimum. However, once you push a little and distort the underlying structure, it would be easy to push until it reaches a point where the ball's material starts "pushing back" and the force required to push down would grow quickly; this last phenomenon is because the microscopic cells are being deformed substantially.

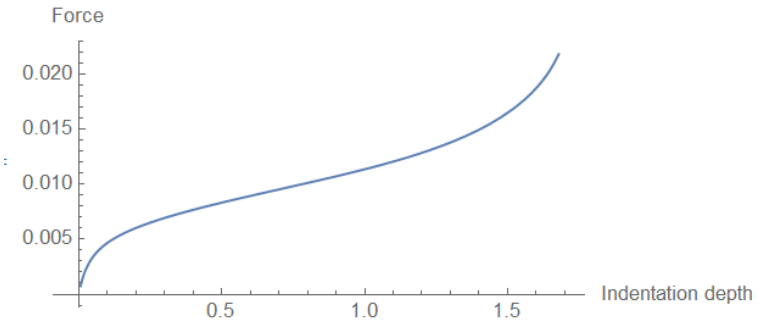

Figure 3: Force-indentation depth curve for initial conditions $b_0 = 0, \upsilon$ = 0.25, and arbitrary values of L and Y. Force grows with indentation depth.

To verify the validity of our method, we compared it to published experimental data. The first data set we looked at was "Measurement of Young's Modulus of Vocal Folds by Indentation" by Dinesh Chhetri, Zhaoyan Zhang, and Juergen Neubauer [6]. In their paper, the authors performed indentation tests using a range of indenter diameters on single and double layer silicone rubber models with a range of cover layer thicknesses with known geometry and Young's moduli in order to assess accuracy of the indentation method for stiffness measurements and to estimate the Young's modulus of the vocal fold. However, the important element for our research is their experimentation using point forces on an object and determination of the force curves of the system. We were able to digitize their data and compare it to our theoretical force curves (Figure 4). For this experiment, we used Y = .05 kpa, L = 35 μm, υ = 0.25 and $b_0 = 0.4$. As shown in Figure 4, the curves are not a perfect match. There is little discrepancy until the end of the model. As the conditions for their materials are unknown, the exact constants are unknown as well. However, for the assumptions made this is a fairly good match. At the beginning of the indentation, the curves are both nearly linear and largely identical. At large indentation depths, the curves diverge as the theoretical curve grows polynomialy. One issue that arose in our data is that we did not have their values for the Young's Modulus, length, or υ. The materials that are of interest are often so complex and small that literature values of Y are not available. A

measurement of Y requires a combination of stress-strain analysis. Therefore, we obtained these values ourselves by fitting our model to the experimental curves.

The next data set we looked at was "On the Determination of Elastic Moduli of Cells by AFM Based Indentation" by Yue Ding, Guang-Kui Xu, and Gang-Feng Wang [7]. In their paper, they note that various studies indicate that the cell is supposed to be linearly elastic within small ranges of strain based on analysis of AFM indentation data. However, this study does not account for the influences of large deformations and surface tension in cells. Their goal was to determine the scale of these influences on the elasticity of cells (Figure 5). Again, the original conditions were unknown. Therefore, we adjusted our model by floating the variables Y, L, υ, and b_0 to best approximate experimental conditions. For this experiment, we used Y = .0001 kpa, L = 8.4 μm, υ = 0.25, and $b_0 = 0.4$. When comparing this data to the theoretical model, there were similar issues as with the previous data set. As shown in Figure 5, the data is not a perfect fit. However, both curves are nearly linear at the onset of the experiment. At the end, the theoretical model begins to grow polynomialy while the experimental model stops. While it can be assumed the experiment did not reach this point in indenting the material, this is just speculation and can only be determined by conducting physical experiments on objects with known constants.

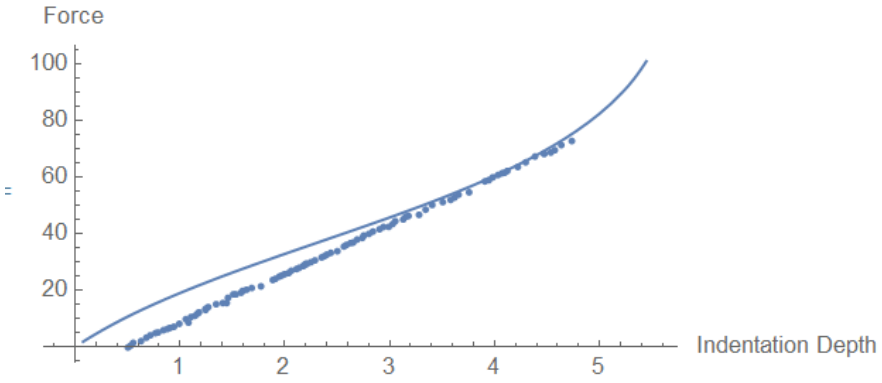

Figure 4: Comparison between our theoretical model (solid line) and an experimental model (dotted line) (see [6]). For this experiment, the model was set to Y = .05 kpa, L = 35 μm, υ = 0.25, and $b_0 = 0.4$.

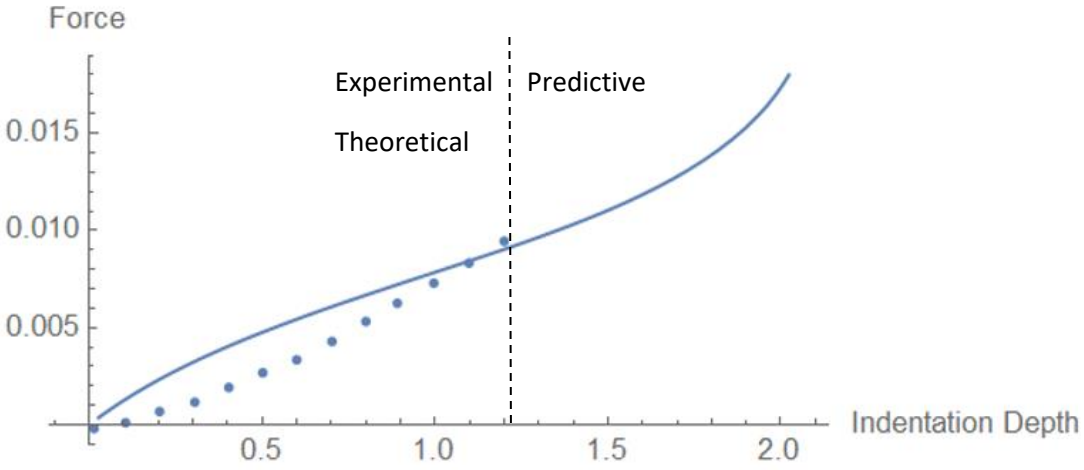

Figure 5: Comparison between the experimental data (dotted line) (see [7]) compared to the proposed theoretical model (solid line). Since the original conditions are unknown, we adjusted our model by playing with the variables Y, L, υ, and b_0. For this experiment, Y = .0001 kpa, L = 8.4 μm, υ = 0.25 and $b_0 = 0.4$.

Conclusions

In this paper we determine that our theoretical model aligns closely with independent experimental data. Our theoretical model supports calculating the energy and the force of cell deformations of spheroidal objects. One issue that arose with our comparisons is the speculation necessary, as we did not know the materials other groups used in their experiments. One way we may improve this comparison in the future would be by conducting deformation tests with known materials to determine values for the various constants. This would ensure that we can accurately prove our model by testing it against known data.

Bibliography

[1] LeClaire, Michael, et al. “A Review of the Biomechanical Properties of Single Extracellular Vesicles.” *Nano Select*, vol. 2, no. 1, 2020, pp. 1–15., doi:10.1002/nano.202000129.

[2] Boys, Alexander J., and Róisín M. Owens. “Measuring Cellular Contraction: Current Progress and a Future in Bioelectronics.” *AIP Publishing*, AIP Publishing LLCAIP Publishing, 1 Apr. 2021, aip.scitation.org/doi/10.1063/5.0040953.

[3] Hooke, R. (1678). *Lectures de potentia restitutiva or of spring explaining the power of springing bodies*.

[4] Timoshenko, S. and Goodier, J. N.: Theory of elasticity, McGraw-Hill, New York, 1951

[5] R.C. Yates (1952). "Cardioid". A Handbook on Curves and Their Properties. Ann Arbor, MI: J. W. Edwards

[6] Chhetri, Dinesh K., et al. “Measurement of Young's Modulus of Vocal Folds by Indentation.” *Journal of Voice*, vol. 25, no. 1, 2011, pp. 1–7., doi:10.1016/j.jvoice.2009.09.005.

[7] Ding, Yue, et al. “On the Determination of Elastic Moduli of Cells by AFM Based Indentation.” *Scientific Reports*, vol. 7, no. 1, 2017, doi:10.1038/srep45575.

Appendix

```
In[ ]:= Clear["Global`*"]
```

Building the Shape of the object

These equations are the initial conditions for the shape of the Cardioid that we deformed. As discussed in the Theory section in the report, the shape is a function of A, θ and ϕ, while b is the indentation Parameter for the system.

```
In[ ]:= r = L (2 a Sin[θ] (1 + b a Cos[θ]));
        r1 = r * Cos[ϕ];
        r2 = r * Sin[ϕ];
        z = L (2 (1 + b a) - 2 a Cos[θ] (1 + b a Cos[θ]) + 2 a b (a - 1));
        jacobian = Simplify[Det[{{D[r1, a], D[r1, θ], D[r1, ϕ]},
                                 {D[r2, a], D[r2, θ], D[r2, ϕ]},
                                 {D[z, a], D[z, θ], D[z, ϕ]}}]];

In[ ]:= volume = Simplify[-∫_0^1 ∫_0^π ∫_0^(2 π) jacobian dϕ dθ da]

Out[ ]= 32/3 (1 + b^2) L^3 π
```

The area in three dimensions it is $\int_0^a \int_0^{\Theta} \int_0^{\phi} \mathrm{J}\, d\phi\, d\Theta\, da$

In this system, the volume of the Jacobian should return L^3, or the volume of the object. Since we do not, we first calibrate the system by dividing each vector dimension by the Jacobian volume and readjust our initial conditions

The area in three dimensions it is $\int_0^a \int_0^{\Theta} \int_0^{\phi} \mathrm{J}\, d\phi\, d\Theta\, da$

```
In[ ]:= r11 = Simplify[r1 / (32/3 (1 + b^2) 1^3 π)^(1/3)]; r22 = Simplify[r2 / (32/3 (1 + b^2) 1^3 π)^(1/3)];

        z11 = Simplify[z / (32/3 (1 + b^2) 1^3 π)^(1/3)];
        JNew = Simplify[Det[{{D[r11, a], D[r11, θ], D[r11, ϕ]},
                             {D[r22, a], D[r22, θ], D[r22, ϕ]},
                             {D[z11, a], D[z11, θ], D[z11, ϕ]}}]];
        Checking = -∫_0^1 ∫_0^π ∫_0^(2 π) JNew dϕ dθ da

Out[ ]= L^3
```

Here we recheck and now see our calibration was correct and that our volume is L^3, which is how we wanted to build the system

Stresses and Strains

Now we begin calculating the stresses and strains of the system. As discussed, the stresses originally are calculated using the change in position in the deformation using the following relationship:

Rx = $R\,(b = b) - R(b = b_0)$

From this will have the various R_i and system of equations for our model

```
In[ ]:= r10 = r11 /. b → b0;
Rx = Simplify[r11 - r10];
r20 = r22 /. b → b0;
Ry = Simplify[r22 - r20];
z10 = z11 /. b → b0;
Rz = Simplify[z11 - z10];
```

Here, we solve for the various Epsilons and Gammas by using Cramer's rule where

$$\begin{pmatrix} D_{i1} \\ D_{i2} \\ Di_3 \end{pmatrix} = \begin{pmatrix} X_1 & Y_1 & Z_1 \\ X_2 & Y_2 & Z_2 \\ X_3 & Y_3 & Z_3 \end{pmatrix}$$

Our notation redefines the initial conditions to be X, Y and Z, instead of r11, r22 and z11

We then take the derivative with respect to each individual variable and then take Cramer's rule for linear equations to solve for ε and γ

We do this due to the fact that we originally defined R as a function of (x,y,z) when it is actually more naturally given in deformed spherical coordinates a, θ and ϕ.

```
x = r11; y = r22; zfinal = z11;
a1 = D[x, a]; a2 = D[x, θ]; a3 = D[x, ϕ];
b1 = D[y, a]; b2 = D[y, θ]; b3 = D[y, ϕ];
c1 = D[zfinal, a]; c2 = D[zfinal, θ]; c3 = D[zfinal, ϕ];
dx1 = D[Rx, a]; dx2 = D[Rx, θ]; dx3 = D[Rx, ϕ];
dy1 = D[Ry, a]; dy2 = D[Ry, θ]; dy3 = D[Ry, ϕ];
dz1 = D[Rz, a]; dz2 = D[Rz, θ]; dz3 = D[Rz, ϕ];
```

dd is the base Jacobian case we divide everything by

```
dd = -Simplify[Det[{{a1, b1, c1}, {a2, b2, c2}, {a3, b3, c3}}]];
```

The following is to solve for the ε structures

```
dxx = Simplify[Det[{{dx1, b1, c1}, {dx2, b2, c2}, {dx3, b3, c3}}]];

dyy = Simplify[Det[{{a1, dy1, c1}, {a2, dy2, c2}, {a3, dy3, c3}}]];

dzz = Simplify[Det[{{a1, b1, dz1}, {a2, b2, dz2}, {a3, b3, dz3}}]];
```

The following is for the γ structures

```
dxy = Simplify[Det[{{a1, dx1, c1}, {a2, dx2, c2}, {a3, dx3, c3}}]]; dxz = Simplify[Det[{{a1, b1, dx1}, {a2, b2, dx2}, {a3, b3, dx3}}]];

dzy = Simplify[Det[{{a1, dz1, c1}, {a2, dz2, c2}, {a3, dz3, c3}}]]; dzx = Simplify[Det[{{dz1, b1, c1}, {dz2, b2, c2}, {dz3, b3, c3}}]];

dyz = Simplify[Det[{{a1, b1, dy1}, {a2, b2, dy2}, {a3, b3, dy3}}]]; dyx = Simplify[Det[{{dy1, b1, c1}, {dy2, b2, c2}, {dy3, b3, c3}}]];
```

Epsilon

This is how we construct the various ε_i

In[ ]:=

```
εx = dxx/dd;
εy = dyy/dd;
εz = dzz/dd;
```

Gamma

This is how we construct the various γ_{ij}

$$\gamma xy = \text{Simplify}\left[\frac{dxy}{dd} + \frac{dyx}{dd}\right];$$

$$\gamma xz = \text{Simplify}\left[\frac{dxz}{dd} + \frac{dzx}{dd}\right];$$

$$\gamma yz = \text{Simplify}\left[\frac{dyz}{dd} + \frac{dzy}{dd}\right];$$

Now that we have the various γ's and ε's, we can construct the strain vector $\vec{\varepsilon}$. Additionally, we build the matrices λ, μ and D so that we can calculate σ. Δ is used in place of D due to Mathematica typeset notation already having a set value for D, that being the derivative function. Traditionally, the standard notation for Young's modulus is E. However, due to Mathematica typeset notation already having a set value of E, we use the lesser used notation of Y to symbolize Young's Modulus.

$$\lambda = \frac{Y\,\nu}{(1+\nu)\,(1-2\,\nu)};\quad \mu = \frac{Y}{2\,(1+\nu)};$$

$$\Delta = \begin{pmatrix} \lambda+2\mu & \lambda & \lambda & 0 & 0 & 0 \\ \lambda & \lambda+2\mu & \lambda & 0 & 0 & 0 \\ \lambda & \lambda & \lambda+2\mu & 0 & 0 & 0 \\ 0 & 0 & 0 & \mu & 0 & 0 \\ 0 & 0 & 0 & 0 & \mu & 0 \\ 0 & 0 & 0 & 0 & 0 & \mu \end{pmatrix};$$

$$\varepsilon = \begin{pmatrix} \varepsilon x \\ \varepsilon y \\ \varepsilon z \\ \gamma yz \\ \gamma xz \\ \gamma xy \end{pmatrix};$$

Now we begin to build the energy integral. We take the transpose between the dot product of ε and σ and simplify it.

$$D1 = \text{Simplify}\left[\frac{((\text{Transpose}[\varepsilon].(\Delta.\varepsilon))[[1]][[1]])\ (dd)}{2}\right];$$

Now we take the integrals. In theory, this is $\frac{1}{2}\int_0^{\pi}\int_0^{1}\int_0^{2\pi}(\sigma.\varepsilon)\,d\phi\,da\,d\theta$. In the following lines, we calculate the integrals step by step for the purpose of having shorter computer runtimes

```
In[ ]:= D3 = Integrate[D1, {θ, 0, π}, Assumptions → {0 < b < 1, 0 < a < 1, 1 / 2 > ν > 0}];
```

```
In[ ]:= D4 = Integrate[D3, {a, 0, 1}, Assumptions → {0 < b < 1, 1 / 2 > ν > 0}];
```

```
In[•]:= Energy = FullSimplify[2 * Integrate[D4, {ϕ, 0, π}, Assumptions → {0 < b < 1, 1 / 2 > ν > 0}]]
```

$$
\begin{aligned}
\text{Out}[\bullet]= -\Big(\Big(L^3\,Y\,\Big(8\,b\,\Big(6\,b\,\left(1+b^2\right)^{2/3}\,b0\,(679-121\,\nu)+768\,b^5\,\left(1+b^2\right)^{1/3}\,b0\,\Big(\left(1+b^2\right)^{1/3}-2\,\left(1+b0^2\right)^{1/3}\Big)\,(1+\nu)+\\
384\,b^6\,\left(1+b0^2\right)^{1/3}\,\left(-2\,\left(1+b^2\right)^{1/3}+3\,\left(1+b0^2\right)^{1/3}\right)\,(1+\nu)+16\,b^3\,\left(1+b^2\right)^{2/3}\,b0\,(59+112\,\nu)+\\
3\,\left(1+b^2\right)^{2/3}\,b0^2\,(-679+121\,\nu)-b^2\,\left(1+b^2\right)^{2/3}\,\left(2037-363\,\nu+8\,b0^2\,(59+112\,\nu)\right)+\\
8\,b^4\,\Big(85\,\left(1+b^2\right)^{2/3}+16\,\Big(-18\,\left(1+b^2\right)^{1/3}\,\left(1+b0^2\right)^{1/3}+9\,\left(1+b0^2\right)^{2/3}+2\,\left(1+b^2\right)^{2/3}\,\nu-\\
18\,\left(1+b^2\right)^{1/3}\,\left(1+b0^2\right)^{1/3}\,\nu+9\,\left(1+b0^2\right)^{2/3}\,\nu+3\,\left(1+b^2\right)^{2/3}\,b0^2\,(1+\nu)\Big)\Big)\Big)-\\
6\,\left(1+b^2\right)^{2/3}\,(b-b0)^2\,\left(281+768\,b^2\,\left(-2+b^2\right)\,(-1+\nu)+889\,\nu\right)\,\text{ArcTanh}[b]-\\
3\,\left(1+b^2\right)^{2/3}\,(b-b0)^2\\
\left(96\,b^4\,(-1+\nu)+9\,\sqrt{9+16\,b^2}\,(37+5\,\nu)-8\,b^2\,\left(135-14\,\sqrt{9+16\,b^2}+5\,\sqrt{9+16\,b^2}\,\nu\right)\right)\\
\text{Log}\left[-1-4\,b+\sqrt{9+16\,b^2}\right]+3\,\left(1+b^2\right)^{2/3}\,(b-b0)^2\\
\Big(\Big(96\,b^4\,(-1+\nu)-9\,\sqrt{9+16\,b^2}\,(37+5\,\nu)+8\,b^2\,\left(-135-14\,\sqrt{9+16\,b^2}+5\,\sqrt{9+16\,b^2}\,\nu\right)\Big)\\
\text{Log}\left[1-4\,b+\sqrt{9+16\,b^2}\right]+\Big(96\,b^4\,(-1+\nu)+9\,\sqrt{9+16\,b^2}\,(37+5\,\nu)-\\
8\,b^2\,\left(135-14\,\sqrt{9+16\,b^2}+5\,\sqrt{9+16\,b^2}\,\nu\right)\Big)\,\text{Log}\left[-1+4\,b+\sqrt{9+16\,b^2}\right]+\\
\left(-96\,b^4\,(-1+\nu)+9\,\sqrt{9+16\,b^2}\,(37+5\,\nu)+8\,b^2\,\left(135+14\,\sqrt{9+16\,b^2}-5\,\sqrt{9+16\,b^2}\,\nu\right)\right)\\
\text{Log}\left[1+4\,b+\sqrt{9+16\,b^2}\right]\Big)\Big)\Big)\Big/\\
\left(6144\,b^5\,\left(1+b^2\right)\,\left(1+b0^2\right)^{2/3}\,(1+\nu)\,(-1+2\,\nu)\right)\Big)
\end{aligned}
$$

Now we have the energy. Since it is in terms of b, we now convert it into terms of S. In order to do this we first define S in terms of B and then Solve for B in terms of S.
First we get S by getting its parameters at the total boundary of the system

```
In[•]:= FullSimplify[{r11, r22, z11} /. {a → 1, θ → π}]
```

$$
\text{Out}[\bullet]= \left\{0,\ 0,\ \frac{L\,\left(\frac{6}{\pi}\right)^{1/3}}{\left(1+b^2\right)^{1/3}}\right\}
$$

Now since we do the initial indentation-final indentation, we have $S(b_0) - S(b)$ and solve for b

```
In[•]:= Solve[S == L (6/π)^(1/3) / (1 + b0^2)^(1/3) - L (6/π)^(1/3) / (1 + b^2)^(1/3), b][[2]]
```

$$
\text{Out}[\bullet]= \left\{b \to \frac{\sqrt{-3+\frac{18\,L^3}{\pi\,\left(L\,\left(\frac{6}{\pi}\right)^{1/3}-\left(1+b0^2\right)^{1/3}\,S\right)^3}+\frac{18\,b0^2\,L^3}{\pi\,\left(L\,\left(\frac{6}{\pi}\right)^{1/3}-\left(1+b0^2\right)^{1/3}\,S\right)^3}}}{\sqrt{3}}\right\}
$$

Using this, we now put the energy in terms of S. We copy and paste the result of the Energy below (ES) to save on runtime issues.

In[•]:=
```
ES =
 -(((L^3 Y
      (8 b (6 b (1 + b^2)^(2/3) b0 (679 - 121 ν) + 768 b^5 (1 + b^2)^(1/3) b0 ((1 + b^2)^(1/3) - 2 (1 + b0^2)^(1/3)) (1 + ν) +
           384 b^6 (1 + b0^2)^(1/3) (-2 (1 + b^2)^(1/3) + 3 (1 + b0^2)^(1/3)) (1 + ν) +
           16 b^3 (1 + b^2)^(2/3) b0 (59 + 112 ν) + 3 (1 + b^2)^(2/3) b0^2 (-679 + 121 ν) -
           b^2 (1 + b^2)^(2/3) (2037 - 363 ν + 8 b0^2 (59 + 112 ν)) +
           8 b^4 (85 (1 + b^2)^(2/3) + 16 (-18 (1 + b^2)^(1/3) (1 + b0^2)^(1/3) + 9 (1 + b0^2)^(2/3) +
                 2 (1 + b^2)^(2/3) ν - 18 (1 + b^2)^(1/3) (1 + b0^2)^(1/3) ν + 9 (1 + b0^2)^(2/3) ν +
                 3 (1 + b^2)^(2/3) b0^2 (1 + ν)))) -
        6 (1 + b^2)^(2/3) (b - b0)^2 (281 + 768 b^2 (-2 + b^2) (-1 + ν) + 889 ν) ArcTanh[b] -
        3 (1 + b^2)^(2/3) (b - b0)^2 (96 b^4 (-1 + ν) + 9 Sqrt[9 + 16 b^2] (37 + 5 ν) -
           8 b^2 (135 - 14 Sqrt[9 + 16 b^2] + 5 Sqrt[9 + 16 b^2] ν)) Log[-1 - 4 b + Sqrt[9 + 16 b^2]] +
        3 (1 + b^2)^(2/3) (b - b0)^2
         ((96 b^4 (-1 + ν) - 9 Sqrt[9 + 16 b^2] (37 + 5 ν) + 8 b^2 (-135 - 14 Sqrt[9 + 16 b^2] + 5 Sqrt[9 + 16 b^2] ν))
            Log[1 - 4 b + Sqrt[9 + 16 b^2]] +
           (96 b^4 (-1 + ν) + 9 Sqrt[9 + 16 b^2] (37 + 5 ν) - 8 b^2 (135 - 14 Sqrt[9 + 16 b^2] + 5 Sqrt[9 + 16 b^2] ν))
            Log[-1 + 4 b + Sqrt[9 + 16 b^2]] +
           (-96 b^4 (-1 + ν) + 9 Sqrt[9 + 16 b^2] (37 + 5 ν) + 8 b^2 (135 + 14 Sqrt[9 + 16 b^2] - 5 Sqrt[9 + 16 b^2] ν))
            Log[1 + 4 b + Sqrt[9 + 16 b^2]])))) / (6144 b^5 (1 + b^2) (1 + b0^2)^(2/3) (1 + ν) (-1 + 2 ν)));

ESS = ES /. b → Sqrt[-3 + 18 L^3 / (π (L (6/π)^(1/3) - (1 + b0^2)^(1/3) S)^3) + 18 b0^2 L^3 / (π (L (6/π)^(1/3) - (1 + b0^2)^(1/3) S)^3)] / Sqrt[3];

b1 = Sqrt[-3 + 18 L^3 / (π (L (6/π)^(1/3) - (1 + b0^2)^(1/3) S)^3) + 18 b0^2 L^3 / (π (L (6/π)^(1/3) - (1 + b0^2)^(1/3) S)^3)] / Sqrt[3];
```

We now have the Energy defined by the deformation S and not b. We run a simple plot to ensure it works. We can set L, Y, *v* and b_0 as numerical values since they are all constants defined either by the material (Y and *v*), object you are working with (L) or the initial position of the stress (b_0).

In[•]:=
```
L = 1; Y = 1; ν = .01; b0 = .0;
Plot[ESS, {S, 0, .2}, {PlotRange → All}]
```

Out[•]=

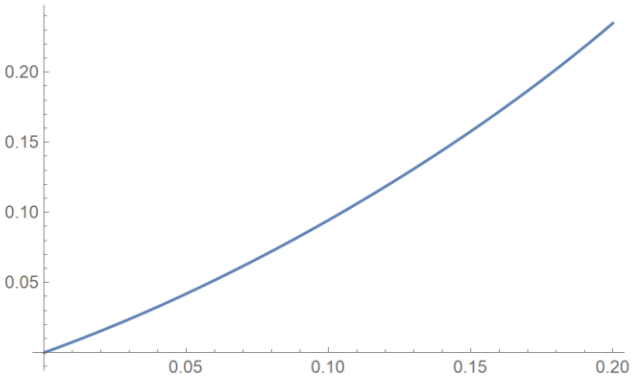

Now that we have the energy, we calculate can compute the Force. The force is defined as $F = \frac{-\partial E}{\partial x}$. However, due to the Energy not really being in terms of S, solve by taking $\frac{\partial E}{\partial b}\frac{\partial b}{\partial S}$.

```
In[ ]:= dbds = D[ Sqrt[-3 + 18 L^3/(π (L (6/π)^(1/3) - (1+b0^2)^(1/3) S)^3) + 18 b0^2 L^3/(π (L (6/π)^(1/3) - (1+b0^2)^(1/3) S)^3)] / Sqrt[3], S];

dESdb = D[ES, b] /. b → Sqrt[-3 + 18 L^3/(π (L (6/π)^(1/3) - (1+b0^2)^(1/3) S)^3) + 18 b0^2 L^3/(π (L (6/π)^(1/3) - (1+b0^2)^(1/3) S)^3)] / Sqrt[3];

F = -dESdb * dbds;
```

The solution for the force is suppressed due to it being incredibly long and difficult to simplify. However, the expression is not important. What is important is that we now have the tools to calculate the Force and Energy for any initial conditions and indentation.

Alternative method

The above method of direct integration for the Energy of the system takes a lot of computing power and takes along time to run. We also developed a numerical method of integration to calculate the Energy.

```
In[ ]:= b0 = 0;
deriv = {}
Do[
 tablenub = {};
 Do[
  UI = 2 π * NIntegrate[D3 /. {Y → 1, L → 1}, {a, 0.01, 0.99}];
  AppendTo[tablenub, {b, UI}];
  , {b, (b0 + .001), 1.0, 0.01}];
 h = Interpolation[tablenub];
 dh = D[h[B], B];
 deriv = AppendTo[deriv, {v, dh}];
 , {v, 0.1, 0.4, .05}]
```

This method takes over after the first integral in θ, which is fairly quick to run. It takes the numeric integral over a. Then we multiply by 2π, as that is what the integral in ϕ is in its totality. We then take the function from b0 to 1 (the maximum value of b). We interpolate over b to get the numeric integral. Then at the end, we take solve for each one for terms of v, so that once we have solved for each individual b, we do not need to resolve for v.

The one interesting note for this method is that you must set each constant value. You must set b_0, Y and L, otherwise this method takes way too long. However, since the runtime is short, you can get the results rather quickly.

Using this method, one can now plot the energy or force for the system. An example for the force using the above code is shown below:

```
ParametricPlot[{S, deriv[[4]][[2]] dbds}, {B, (b0 + .001), 1}, AspectRatio → 1 / 2,
 AxesOrigin → {0, 0}]
```

Out[ ]=

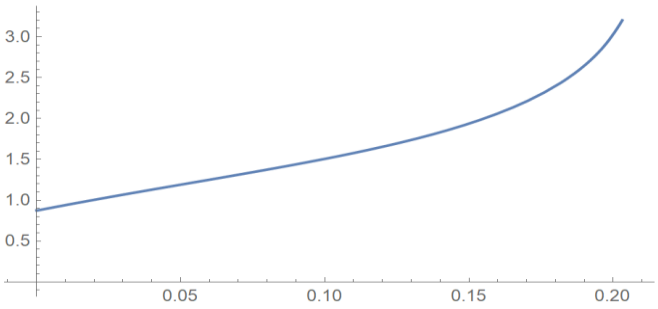

In the term deriv[[4]][[2]], the second term [[2]] must remain so to show the output. The first term (in this case [[4]]) is adjustable for the various values of *v*. It calls the variables from the interpolation function such that deriv[[1]] is *v*=.1, deriv [[2]] is *v*=.15, and so on and so forth.

Plot of the System

The following is a three dimensional plot of the system that can be manipulated to see how the spherical object deforms.

b=0

In[ ]:=
```
Manipulate[
  ParametricPlot3D[{2 a L (1 + a b Cos[θ]) Cos[ϕ] Sin[θ], 2 a L (1 + a b Cos[θ]) Sin[θ] Sin[ϕ],
    L (2 (1 + b a) - 2 a Cos[θ] (1 + b a Cos[θ]) + 2 a b (a - 1))}, {ϕ, 0, 2 π}, {θ, -π, π},
   PlotStyle → {Cyan}], {a, .1, 1}, {b, .1, 1}] /. L → 1
```

Out[ ]=

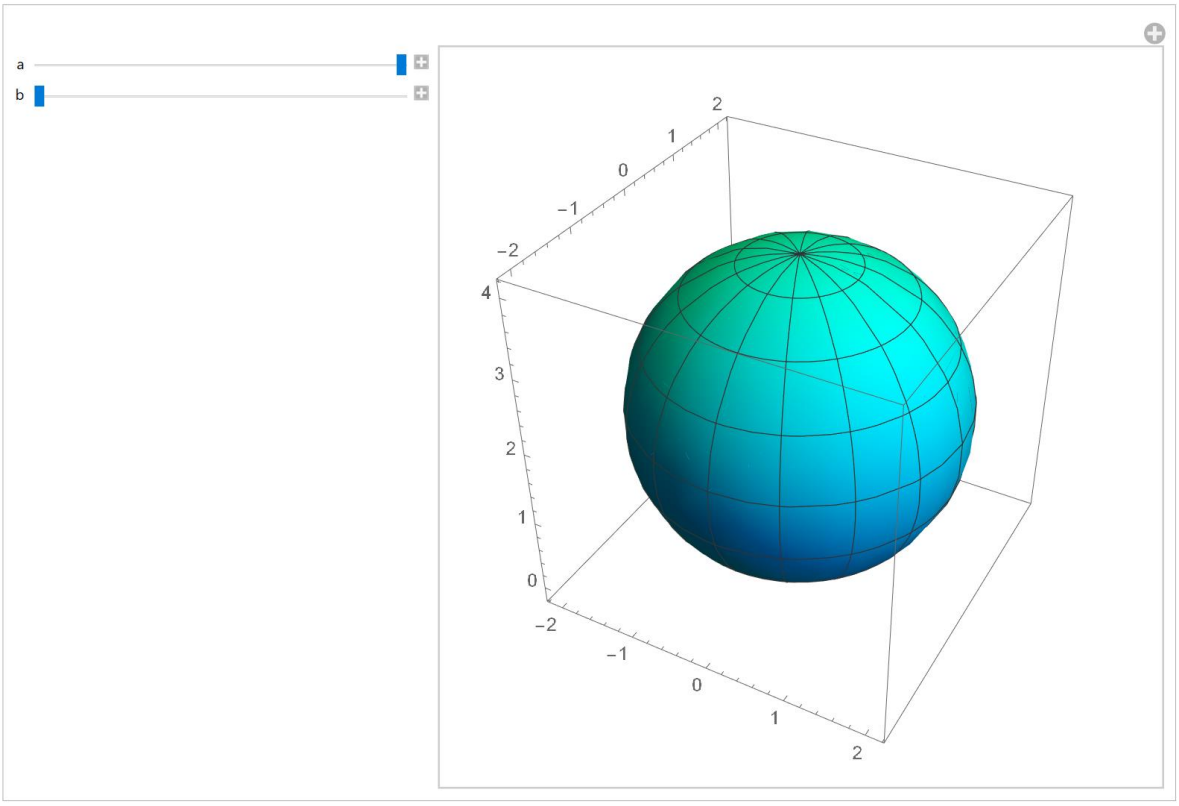

b=.5

```
In[•]:= Manipulate[
  ParametricPlot3D[{2 a L (1 + a b Cos[θ]) Cos[ϕ] Sin[θ], 2 a L (1 + a b Cos[θ]) Sin[θ] Sin[ϕ],
    L (2 (1 + b a) - 2 a Cos[θ] (1 + b a Cos[θ]) + 2 a b (a - 1))}, {ϕ, 0, 2 π}, {θ, -π, π},
   PlotStyle → {Cyan}], {a, .1, 1}, {b, .1, 1}] /. L → 1
```

Out[•]=

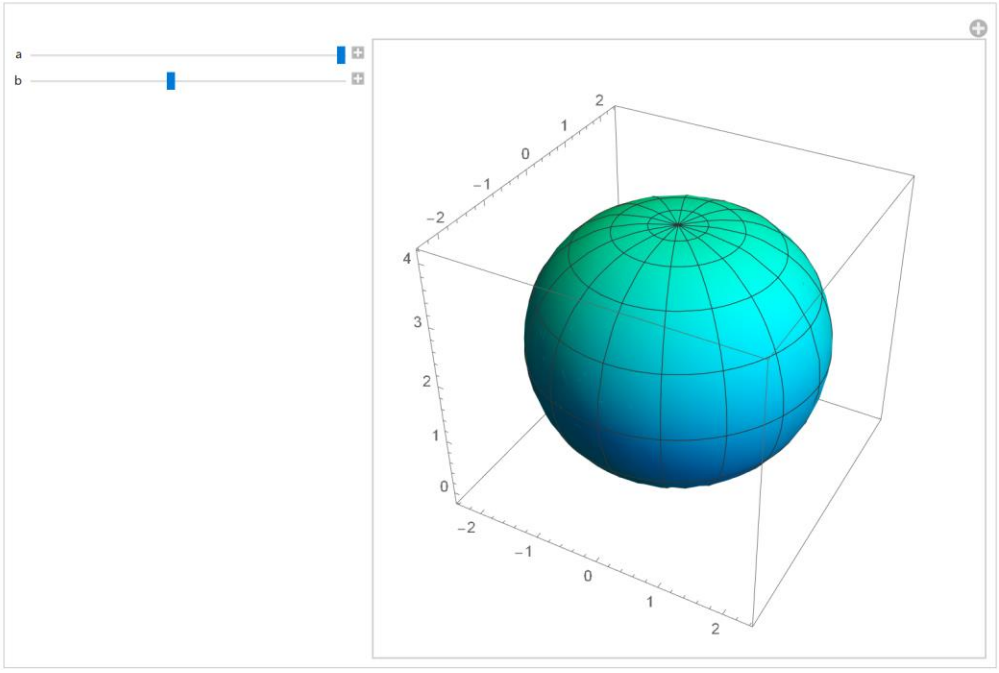

b=1

```
In[•]:= Manipulate[
  ParametricPlot3D[{2 a L (1 + a b Cos[θ]) Cos[ϕ] Sin[θ], 2 a L (1 + a b Cos[θ]) Sin[θ] Sin[ϕ],
    L (2 (1 + b a) - 2 a Cos[θ] (1 + b a Cos[θ]) + 2 a b (a - 1))}, {ϕ, 0, 2 π}, {θ, -π, π},
   PlotStyle → {Cyan}], {a, .1, 1}, {b, .1, 1}] /. L → 1
```

Out[•]=